24th COBEM - 2017

24th ABCM International Congress of Mechanical Engineering
December 3-8, 2017, Curitiba, PR, Brazil.

COBEM-2017-0965
NONLINEAR MODELING, SIMULATION AND CONTROL OF A TWO-WHEELED INVERTED PENDULUM

G. D. Silva
B.L. Pereira
Federal University of Uberlândia , João Naves de Ávila ave., 2121 – Zip Code: 38408-100, Uberlândia-MG, Brazil
brunolp.meca@gmail.com

A. R. Sousa
Federal University of Uberlândia
alexanrsousa@gmail.com.br

L. Sanches
Federal University of Uberlândia
lsanches@ufu.br

J.J.P.Z.S Tavares
Federal University of Uberlândia
jean.tavares@ufu.br

R. H. Murofushi
Federal University of Uberlândia
hiroshirhm@gmail.com

R.N. Cardoso
Federal University of Uberlândia
rodrigonogueira@outlook.com

Abstract. *In the study of nonlinear systems, the modeling process has an important role in the control algorithm's performance. Once the quality of a model is assured, it can be used effectively in control techniques. Inverted pendulum systems' control is a classical issue in this field, and so, improvements in those techniques are usually studied. This work aims to improve the performance of PID and fuzzy controllers by adapting them to a nonlinear model and evaluate them through simulation before applying them to the real system. The nonlinear dynamic model of the two-wheeled inverted pendulum is obtained through the Newton-Euler formulation and the linear model is obtained linearizing the nonlinear model. Normally, due to the nonlinearity of the model's equation, it is impossible to solve them analytically, requiring a numerical approximation. For this purpose, the 4th order Runge-Kutta method was used. In this paper a PID controller using the linear model (LPID) was proposed, and classic PID controller is designed and adapted to the nonlinear model (NLPID). Using a NLPID controller, the simulation and vehicle's response in real time were compared to statistically validate the nonlinear model. Then a simulation was performed comparing the performance of the controllers, as well as the LPID performance for the linear model and the nonlinear model for different sampling times.*

Keywords: *Inverted pendulum, Nonlinear System model, Runge-Kutta method, Fuzzy control, PID control.*

1. INTRODUCTION

The study of control methodologies applied to inverted pendulum is widely performed (Bonafilia, 2014; Chen, Lin and Lin, 2008; Saifizul, 2006) due to the nonlinearity characteristic of the system. Such nonlinear system is commonly used in the benchmarking survey regarding the efficiency of controllers.

There are many works that explore the control of nonlinear systems through the linearization of the system model under study within the operating region (Bonafilia, 2014; Juang and Lum, 2013). However, when performing this

procedure, some of the system's characteristics are neglected, which may reduce the efficiency of the designed controller.

In a recent work, a Fuzzy PD controller was used to control the vertical position and tilt angle of a simulated inverted pendulum (El-Nagar, *et al.*, 2014), whose model considers some non-linearities present in the real system.

Another relevant recent work used a Fuzzy controller associated with a PI controller to simultaneously control the vertical position and the tilt angle (Feifei, *et al.*, 2013). The PI controller was designed through the root locus method based on the linear model. When comparing, in real time, the inverted pendulum's response obtained in both of these works with the simulation, some differences can be observed in these responses which can be attributed to the non-linearities neglected when simulating.

Thus, this paper proposes two distinguished models (nonlinear and linear), simulation and control of a two-wheeled vehicle and analysis of the results for a PID controller with the linear and nonlinear model, verifying the decharacterization that the linearization provokes as the sampling time is increased. In this direction, it compares the performance among three types of controller: a PID whose parameters were obtained from the linearized model LPID, a PID obtained from the LPID control adapted for the nonlinear model NLPID, and a fuzzy controller.

This paper presents the two wheeled dynamic model and the simulation method in section 2, followed by the control method in section 3. Section 4 shows results and discussion, and, section 5 highlight the main concludes conclusion about this the development of the present article.

2. TWO WHEELED DYNAMIC MODEL AND SIMULATION METHOD

A scheme for the two-wheeled inverted pendulum representation is show in Figure 1. In this figure is also represented the free body diagram for the vehicle along with the main forces acting on the vehicle and the coordinates and the reference frame. That information is used in the dynamic modelling section described below.

The primary variables that influence the dynamic behavior of this system and the parameters of the vehicle can be found in tables 1 and 2 respectively, along with their values and their measurement units. The values found in table 2 were obtained through calculation, identification procedures and measurements on the real vehicle.

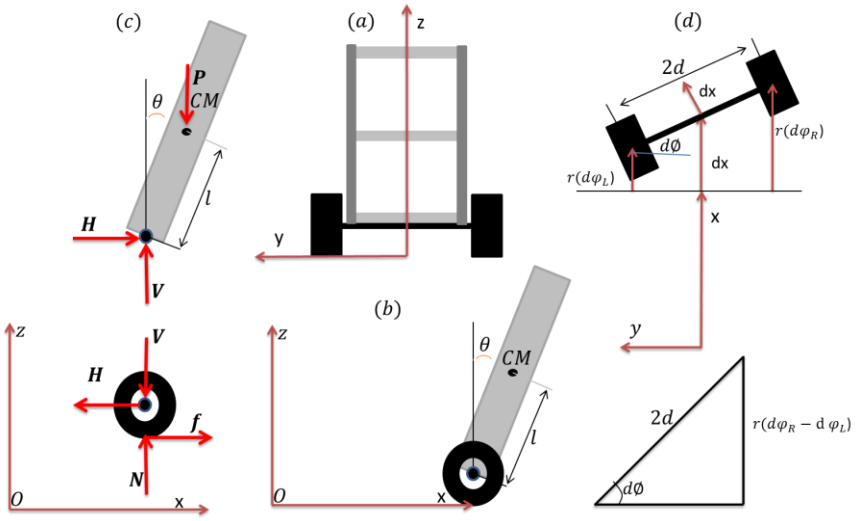

Figure 1. Representation of two-wheeled inverted pendulum. (a) Front view of the vehicle. (b) Coordinates and reference frame. (c) Free body diagram and main forces acting in the vehicle and CG (center of gravity). (d) Relationships between the vehicle's base position and the wheel's rotation, the description of the variables shown is in the Table 1.

Table 1- System variables.

Symbol	Physical interpretation	Unit
θ	Vertical tilt angle of the vehicle	Rad
x	Horizontal position of the vehicle	M
$\emptyset$	Rotation angle around the z axis	Rad
φ_R	Right wheel's rotation angle	Rad
φ_L	Left wheel's rotation angle	Rad

T_R	Right motor torque	Nm
T_L	Left motor torque	Nm
u_R	Control action for the right motor	Dimensionless
u_L	Control action for the left motor	Dimensionless
f	Resulting force on the vehicle	N
H	Horizontal contact force in the wheels axis	N
V	Vertical contact force in the wheels axis	N
N	Normal force with the floor	N
P	Weight of pendulum	N

Table 2- System parameters.

Symbol	Physical interpretation	Value (unit)
J_p	Vehicle's rotational inertia	$48x10^{-4}$ (kg.m²)
J_z	Vehicle's rotational inertia around the z axis	$7{,}18x10^{-3}$ (kg.m²)
J_W	Rotation inertia of the wheels, gear and axis	$3{,}1x10^{-5}$(kg.m^2)
g	Gravity acceleration	9.79 (m/s²)
r	Wheels' radius	0.0316 (m)
M	Mass of the two wheels	0.062 (kg)
m	Mass of the pendulum	1.304 (kg)
d	Half of distance between wheels	0.115 (m)
l	Position of the center of mass	0.0748 (m)
C_a	Dynamic friction in the wheels' axis	0.0005 (kg.m^2/s)
b	Motor's dynamic friction	0.002 (kg.m^2/s)
V_{cc}	Maximum electromotive force in the motor	6 (V)
K_m	Motor's constant of torque	0.5373(Nm/A)
K_e	Motor's constant of counter-electromotive force	0.34 (Vs)
R	Motor's internal resistance	0.9246 (ohm)
dz	Motor's dead zone	0.03 (Dimensionless)

The dynamic modelling was obtained using the Newton-Euler formalism. Initially the vehicle's Center of Gravity (CG) was positioned according to the reference frame (see Figure 1). The relation between the vehicle's base position (x, ϕ) and the angular position of the wheels (φ_R, φ_L) are stated by Eq. (1) and (2).

$$x = (r/2).(\varphi_R + \varphi_L) \tag{1}$$

$$\phi = (r/2d).(\varphi_R - \varphi_L) \tag{2}$$

Using the reference frame shown by Figure 1, the equations that describe the motion of the center of gravity of the suspended part can be inferred as follows (Eq. (3), (4) and (5)). Where Eq. (3) and (4) refer to Newton's 2nd law for an (x, y) position of the suspense part. And the Eq. (5) is Newton's 2nd Law for the vehicle's rotation.

$$m\frac{d^2}{dt^2}(x + l.\sin\theta) = H \tag{3}$$

$$m\frac{d^2}{dt^2}(l.\cos\theta) = V - m.g \tag{4}$$

$$J_p\frac{d^2\theta}{dt^2} = V..l\sin\theta - H.l\cos\theta - C_a(\dot{\theta} - \dot{\varphi}_R) - C_a(\dot{\theta} - \dot{\varphi}_L) \tag{5}$$

The dynamic equation which describes the motion of the two wheeled vehicle's base is shown by Eq. (6).

$$M\frac{d^2x}{dt^2} = f - H \tag{6}$$

The net force applied to the vehicle's base is stated by Eq. (7), and can be understood as the sum of the net force produced by each of the motors, which are generated by the motor's torque minus the inertial effects and dynamic friction inside the motors.

$$f = (1/r).(T_R - J_W\ddot{\varphi}_R - b\dot{\varphi}_R) + (1/r).(T_L - J_W\ddot{\varphi}_L - b\dot{\varphi}_L) \tag{7}$$

A complimentary definition of a "expected force" is given by Eq. (8). This force is the one that would be transmitted to the vehicle's base in the case that there were no friction inside the motor and also if the transmission and wheel inertial moments were negligible.

$$f^* = (T_R + T_L)/r \tag{8}$$

Eq. (9), (10) and (11) can be obtained through inference from Eq. (1) to (8). Those equations describe the behavior of the two wheeled vehicle with respect to its own state variables (x, θ and $\varnothing$). Where the behavior of the angle θ, the x coordinate and the base rotation angle $\varnothing$ are described by Eq. (9), (10) and (11) respectively.

$$(J_P + ml^2)\ddot{\theta} + (ml\cos\theta)\ddot{x} = mlg\sin\theta - 2C_a\dot{\theta} + 2(C_a/r)\dot{x} \tag{9}$$

$$(ml\cos\theta).\ddot{\theta} + (M + m + 2J_W/r^2)\ddot{x} = f^* - (2b/r^2).\dot{x} + ml\sin\theta.\dot{\theta}^2 \tag{10}$$

$$(J_Z + 2(d/r)^2)\ddot{\phi} = (d/r^2).(T_R - T_L) - 2b(d/r)^2\dot{\phi} \tag{11}$$

To perform the simulation, the system of equations composed by Eq. (9), (10) and (11) must be solved regarding the time variable. As these equations are not linear, the solution must be found through numerical techniques, in this case the 4^{th} order Runge Kutta (4RK) method was implemented.

To use the 4RK, the state vector at the instant $t = K\Delta t$ needs to be defined as shown in Eq. (12). The simulation algorithm, which is used for numerical integration using the 4RK method in order to foresee the behavior of the two-wheeled vehicle in the time domain, and follows the structure shown by Eq. (13) until Eq. (18), where the algorithm calculates the temporal derivative of the state vector through Eq. (12) until Eq. (17).

$$r^K = [x, \dot{x}, \theta, \dot{\theta}, \phi, \dot{\phi}]^T_{t=K\Delta t} \tag{12}$$

$$T_R = (K_m/R).(V_{cc}u_R - K_e\dot{\varphi}_R)\mu(|u_R| - dz) \tag{13}$$

$$T_L = (K_m/R).(V_{cc}u_L - K_e\dot{\varphi}_R)\mu(|u_L| - dz) \tag{14}$$

$$\ddot{\theta}_K = \frac{1}{\left(J_p + ml^2 - \frac{(ml\cos(\theta_K))^2}{m + M + 2J_W/r^2}\right)}.\left[-\frac{ml\cos(\theta_K)f^*}{m + M + 2J_W/r^2} + mgl\sin(\theta_K) - \left(2C_a + \frac{m^2l^2\sin(2\theta_K)\dot{\theta}_K}{2\left(m + M + 2J_W/r^2\right)}\right)\dot{\theta}_K + \left(\frac{2C_a}{r} + \frac{(2b/r^2)ml\cos(\theta_K)}{m + M + 2J_W/r^2}\right)\dot{x}_K\right] \tag{15}$$

$$\ddot{x}_K = \frac{1}{m + M + 2J_W/r^2}\left(f^* + ml\sin(\theta_K)(\dot{\theta}_K)^2 - ml\cos(\theta_K)\ddot{\theta}_K - (2b/r^2)\dot{x}_K\right) \tag{16}$$

$$\ddot{\phi}_K = \frac{(T_R - T_L)}{r\left(J_Z + 2(d/r)^2 J_W\right)} \tag{17}$$

$$\dot{r}_K = [\dot{x}, \ddot{x}, \dot{\theta}, \ddot{\theta}, \dot{\phi}, \ddot{\phi}]^T_{t=K\Delta t} \tag{18}$$

For a better understanding, the implemented algorithm can be found in Figures 2 and 3. The Table 3 presents algorithm's parameters. Figure 2 shows the flowchart for the algorithm's main function, which is responsible for the numerical integration and also to organize and display the data obtained through simulation. Figures 3 (a) and (b) shows the flowchart for the Fpend function, which has the information on the system's dynamics, and for the Fcontrol

function, which contains the controller's logic, respectively. The PID and Fuzzy controllers' logic used in simulation are described in the next section.

Using an integration time step of Δt, and a sampling time T_a of 2 ms, a state vector r_0 and the algorithm's framework, one can estimate the next vector state for this simulation.

Table 3. Algorithm's parameters

Symbol	Description
t	time
i	Loop's counting
$K_{1,2,3\ and\ 4}$	RK4's vectors
n_{cycles}	Numbers of sampling cycle
$n_{totalcycles}$	Number of total cycles in time t
n	Number of total cycles in the simulation
u	Action control vector
T_{total}	Total time of the simulation

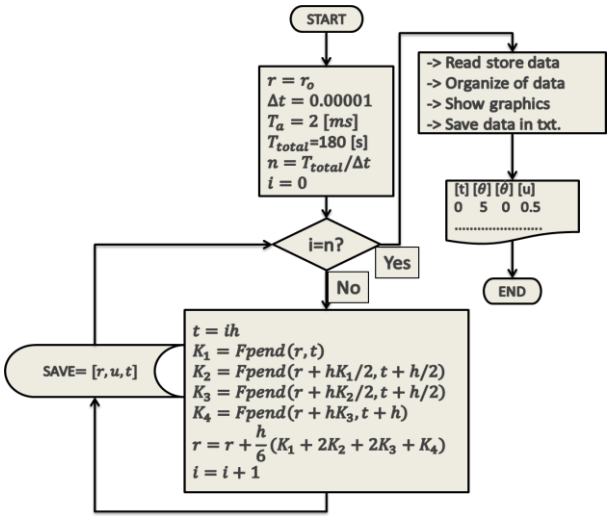

Figure 2. Simplified flowchart of the main function of the algorithm responsible for numerical integration, organize data and show graphics with results of variables of the simulation.

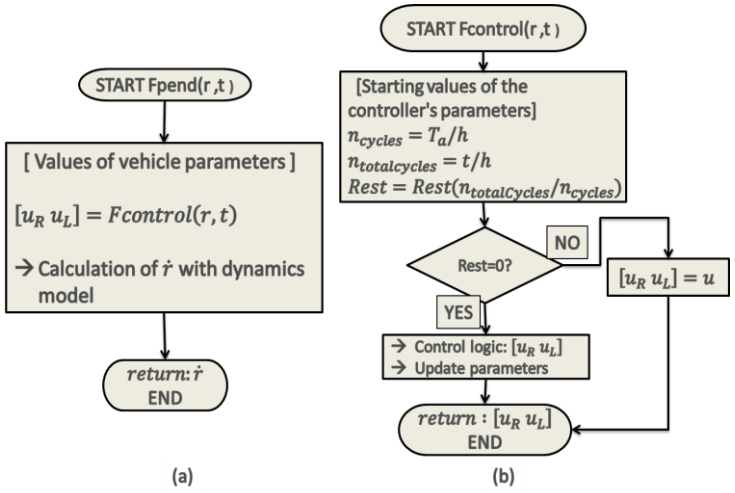

Figure 3. Simplified flowchart of the (a) dynamics function of the vehicle *Fpend* responsible of calculate the temporal derivate of the state vector and (b) Control function for the simulation responsible of control action for the *Fpend*.

3. CONTROL AND IMPROVEMENT OF THE CONTROLLER WITH THROUGH SIMULATION

3.1 PID Controller for the linear model (LPID) .

The LPID controller was obtained through the classical theory of pole placement. For that it was necessary to linearize the method obtained previously through a Taylor series approximation, considering the angles small and supposing low speeds. The calculation of the transfer function for a u input and a θ output was performed through this linear model as shown by Eq. (19) below.

$$G(s) = \frac{-2915s + 0.1891}{s^3 + 654.8s^2 - 180.6s - 51690} \tag{19}$$

Afterwards with assistance from the root locus, a PID controller for an accommodation time of 1.5 second and maximum overshoot of 30% was obtained. The LPID controller was obtained with the constants K_P=1.45, K_D=0.0287 and K_P=41.98 for these project requirements.

3.2 Fuzzy Controller.

The structure of the Fuzzy controller is shown in Figure 4. The input variables considered are: the tilt angle around the vertical axis and the angular speed of the vehicle. The inputs go through a fuzzification process, and then subjected to the inference rules. Fuzzified variables are obtained and, using a trapezoidal defuzzification method and control action u is found.

Figure 4. The structure of Fuzzy controller.

The Fuzzy controller was obtained from the pertinence functions which are expressed in Figure 5. Triangular functions were considered, and the universe of discourse was defined as the tilt angle and the maximum angular speed for sampling interval of 2ms was calculated as around 260°/s. For the control action the 1 and -1 limiting values are upheld.

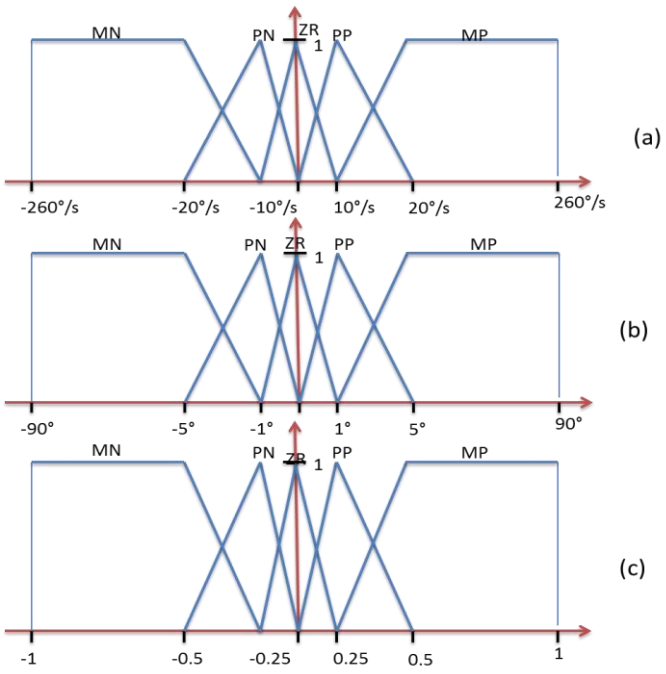

Figure 5. Pertinence functions for (a) angular velocity with vertical, (b) Angle with vehicle and (c) control action for motor, where MP is very positive, PP is poorly positive, ZR is zero, MN is very negative and PN is little negative.

The inference rules for the Fuzzy controller are shown in Table 4. These rules dictate what the values of the linguistic output variables should be according to the linguistic input variables. Using these relations with the pertinence function displayed in Figure 5 for the control action, the defuzzification is performed using the centroid method, and the control action is found.

Table 4. The Fuzzy Control rules. Where MP is very positive, PP is poorly positive, ZR is zero, MN is very negative and PN is little negative.

		$\dot{\theta}$				
	u	MN	PN	ZR	PP	MP
θ	MN	MN	MN	MN	PN	ZR
	PN	MN	MN	PN	ZR	PP
	ZR	MN	PN	ZR	PP	MP
	PP	PN	ZR	PP	MP	MP
	MP	ZR	PP	MP	MP	MP

3.3 PID Controller adapted for the nonlinear model (NLPID)

The flowchart in Figure 6 shows the steps for the controller's parameter enhancement. The initial controller's parameters are saved into a vector *P*. Each of the controller's parameters are assessed individually according to their positions inside the vector. For each parameters two candidates are created, one with a higher value and one with a smaller value. Then the mean squared error is calculated through simulation for the nonlinear model. The flowchart's parameters are shown in Table 5.

If the new parameter produces a smaller squared medium error for the response, it then replaces the previous value and it's saved on vector *P*. The process is repeated for each parameter until the least value for the squared medium error to the nonlinear model is found.

Table 5. Flowchart's parameters.

Symbol	Description
P_m	Candidate parameter to replace the initial parameter
P_m1	Initial parameter with an increment of rate percent
P_m2	Initial parameter minus rate percent
e_{MSEo}	Lower mean squared error
e_{MSEi}	Mean squared error for the parameter P_m

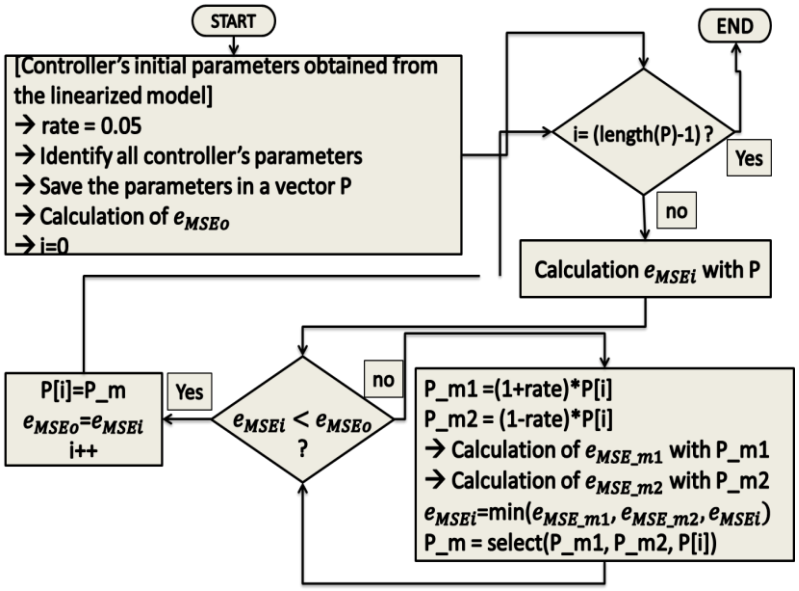

Figure 6. Flowchart to find the PID controller's parameters adapted for the nonlinear model.

4. RESULTS AND DISCUSSIONS

The NLPID controller obtained through the simulation was applied to the vehicle to compare its real time and simulated responses. The responses obtained are shown in Figure 7, where details of the vehicle's transient regime are also displayed. Similarities are observed in both transient and permanent regimens for both responses.

Applying a hypothesis test to the difference between the results, it is verified with a confidence level of 95% that the actual vehicle response and simulation are not different.

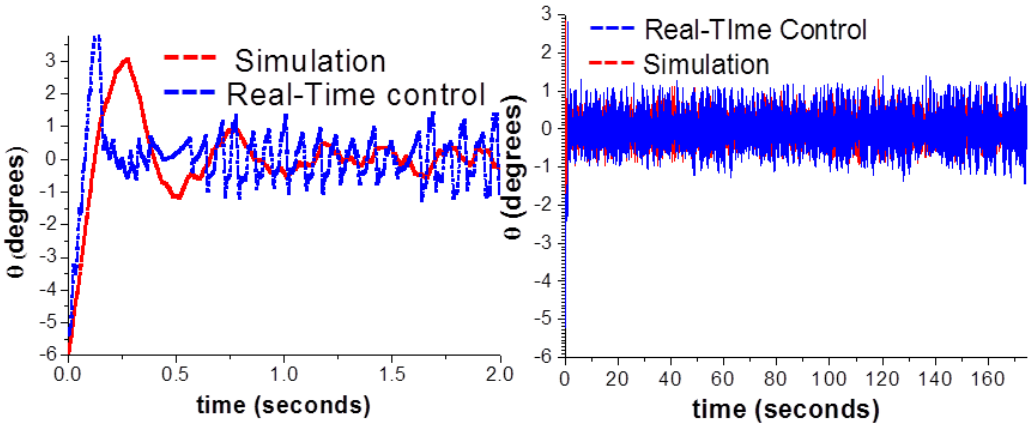

Figure 7. Real-Time control and simulation for vehicle.

The performance of the Fuzzy, NLPID and LPID controllers were compared through simulation using the same starting conditions. The results are shown in Figure 8 together with a discrepancy numerical indicator of each controller. It was observed that the Fuzzy controller presented the lowest discrepancy numerical indicator regarding the vertical position during the entire simulation, followed by the NLPID and LPID controllers.

It is verified with a confidence level of 95% that the use of fuzzy controller ensures lower oscillation of the deviation angle around the reference position when compared to the NLPID controller, which in turn guarantees less oscillation than the LPID controller.

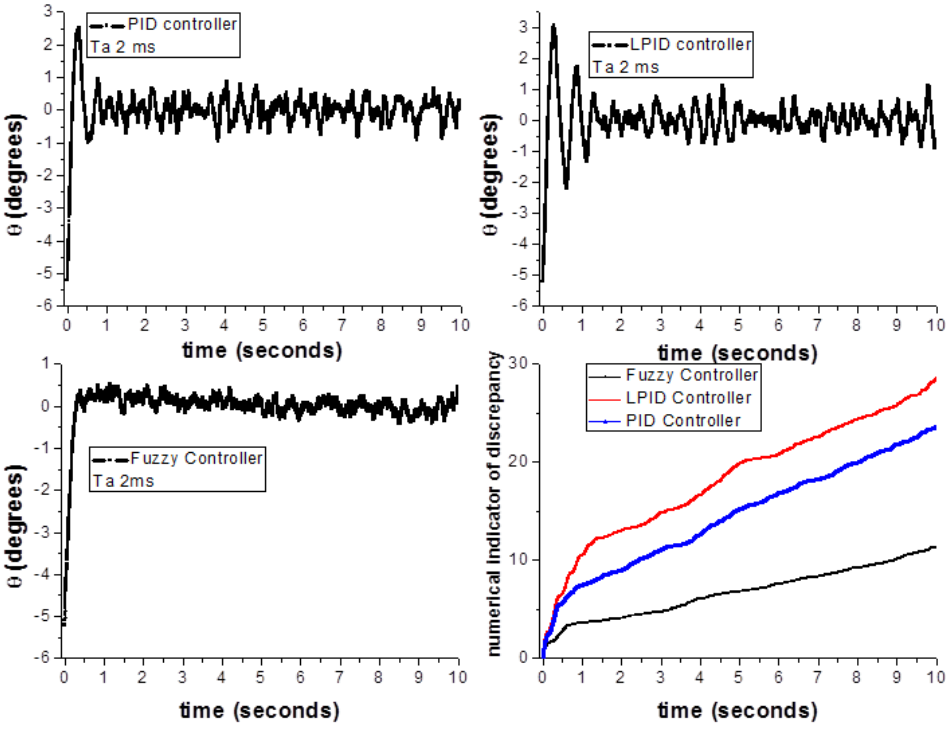

Figure 8. Comparative of the controllers' response performance.

The LPID controller's simulated responses using different sampling times for both linear and nonlinear models are displayed in Figures 9, 10 and 11. It is observed that as the sampling time is increased, the difference between the response for the two models also increase.

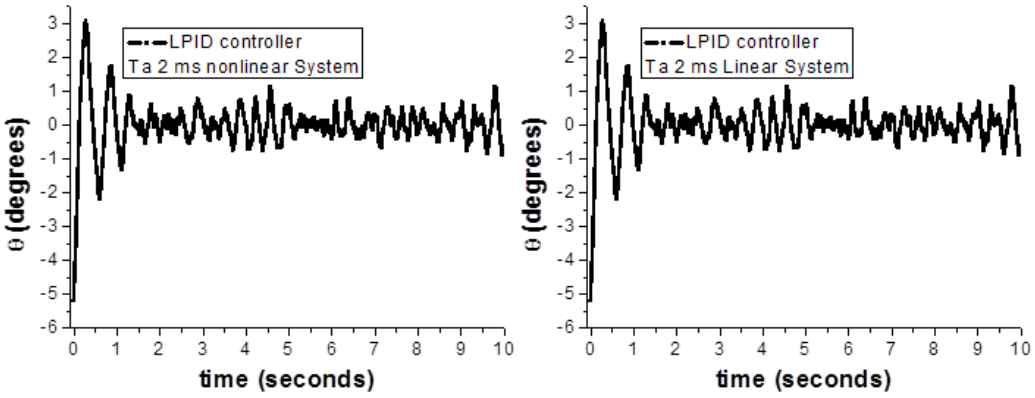

Figure 9. LPID controller's simulated response using linear and nonlinear models the for a sampling time of 2ms.

For a 2ms sampling time, as shown in Figure 9, it is verified with a 95% level of confidence that the mean and variance o the linear and nonlinear models' responses are not different. Corroborating that, Figure 9 does show that the difference between the responses is almost imperceptible. For a 2ms sampling time the controller keeps the tilt angle below 1° and a low angular velocity inside the linearization constraints. That way, the responses of the linear and nonlinear models are considered not different for the same controller.

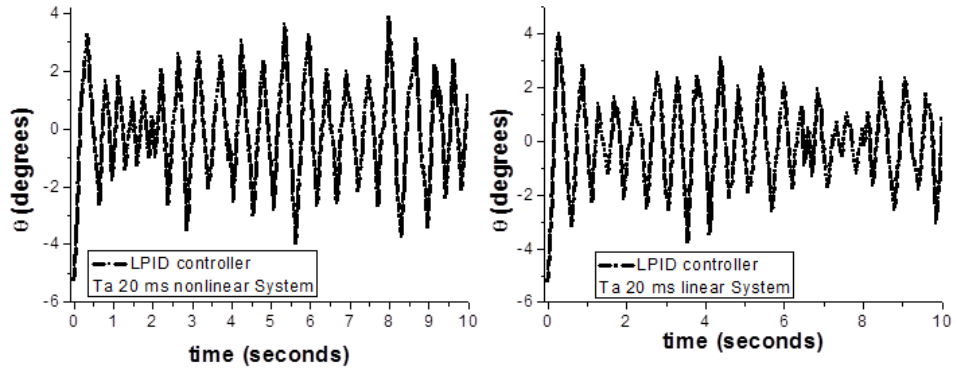

Figure 10. LPID controller's simulated response using linear and nonlinear models the for a sampling time of 20 ms.

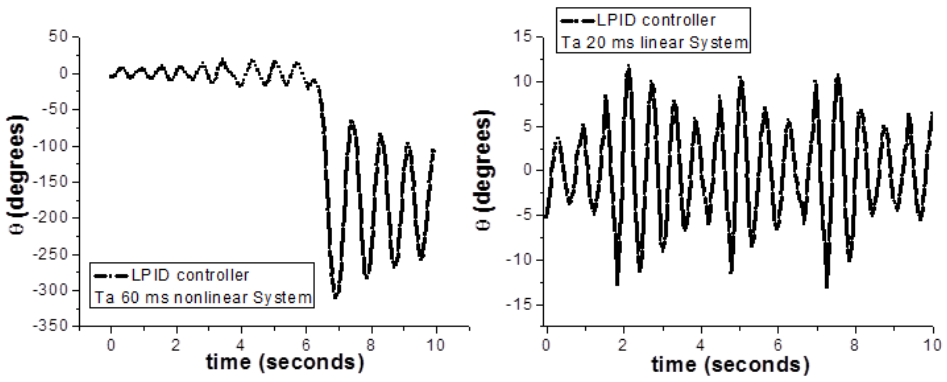

Figure 11. LPID controller's simulated response using linear and nonlinear models the for a sampling time of 60 ms.

The responses for the linear and nonlinear models using the same LPID controller and sampling times of 20ms and 60ms are shown in Figures 10 and 11, respectively. It is verified with a 95% confidence level that for sampling times slower than 20ms the responses for the linear and nonlinear models cannot be considered equal for the same controller.

The biggest differences between the responses for the linear and nonlinear models are observed in Figure 11, and those differences are critical when the sampling time rises to 60ms, where the controller can no longer reject the nonlinearities of the non-linear model due the increase of their effects with the sampling time, although the linear model using the same parameters, even with great oscilation, still mantains a response that varies around the equilibrium position.

5. CONCLUSIONS

The nonlinear model was statistically validated with a confidence level of 95% using he NLPID controller whose parameters were adapted to the nonlinear model.

As the sampling time increases the system distances itself from its linearization condition and thus the nonlinearities begin to become expressive, reaching a breaking point at a sampling time of 60 ms where the controller cannot reject the nonlinearities and can no longer control the system.

The fuzzy controller obtained the best results regarding the minimization of the mean square error of the tilt angle, which is due to the intuition and ability of the fuzzy set theory to incorporate the knowledge of the designer.

The LPID controller was the one that obtained the worst results, due to the fact that, when considering the linearized model, we neglect information from the nonlinear model, especially as it departs from the point of linearization.

Thus, the design of a controller for a nonlinear system should consider the model and sampling time, whose combination may require the adaptation of the control rule, for example, through simulation of the nonlinear model obtained from the real system.

6. ACKNOWLEDGEMENTS

The authors would like to thank CNPq, FAPEMIG and CAPES for supporting this research.

7. REFERENCES

Bonafilia, B., Gustafsson, N. and Nilsson, S., 2014. *Self-balancing two-wheeled robot*. 17 Feb. 2017 <https://pdfs.semanticscholar.org/ad7a/3b833695e8e01c1d41043c75c770276c923c.pdf>.

Chen, C.H., Lin, C.J. and Lin, C.T. , 2008. *Nonlinear System Control Using Adaptive Neural Fuzzy Networks Based on a Modified Differential Evolution, IEEE Transactions on Systems, Man, and Cybernetics — Part C: Aplications and Reviews*, Taiwan,v.39,n.4,p.459-473.

El-Nagar, A. M., El-Bardini, M. and EL-Rabaie, N. M., 2014. *Intelligent control for nonlinear inverted pendulum based on interval type-2 fuzzy PD controller*, Alexandria Engineering Journal 53, 23–32.

Feifei, R., Lei, Z., Le, T., Yanhai, H., and Pengpeng, Z., 2013. *Design and Research of Double Closed- Loop Control Strategy for Inverted Pendulum System*, 3th International Conference on Intelligent System Design and Engineering Applications, China, p. 550 553.

Juang, H.S., Lum, K.Y., 2013. *Design and Control of a Two-Wheel Self-Balancing Robot using the Arduino microcontroller Board*, 10th IEEE International Conference on Control and Automation (ICCA), China, p. 634 639.

Saifizul, A.A. ,2006. *Intelligent Control for Self-erecting Inverted Pendulum Via Adaptive Neuro-fuzzy Inference System*, American Journal of Applied Sciences, Malaysia,v.3,n.4,p.1795-1802,2006.

Zadeh, L.A, 1965. *Fuzzy Sets Information and Control*, Berkeley, v. 8, p. 338-353.

8. RESPONSIBILITY NOTICE

The authors are the only responsible for the printed material included in this paper.